Innovative Infrastructure Solutions (2019) 4:62
https://doi.org/10.1007/s41062-019-0244-x

TECHNICAL PAPERS

Effectiveness of geogrid and its position on the performance of unpaved roads under repetitive loading

K. H. Mamatha[1] · **S. V. Dinesh**[2]

Received: 28 March 2019 / Accepted: 9 October 2019 / Published online: 19 November 2019

Abstract
Road network provides access to communities and plays a vital role in the economic development of a country. These days, the transportation sector is given the utmost importance as premature failures are very common owing to rapid industrialization and urbanization. Also, subgrade failure is a very common scenario in pavement failures. To prevent these failures, geosynthetics have been used widely. In this study, model pavement sections were built in a steel tank with black cotton soil as subgrade forming a weak subgrade layer followed by granular sub-base (GSB) and sacrificial layer at the top. Two biaxial geogrids were considered as reinforcing material, and their position was varied within the GSB layer. The pavement thickness was varied by varying the thickness of GSB. The GSB of thickness 0.25 m, 0.30 m, and 0.35 m were considered. The effectiveness of geogrid on the pavement performance was evaluated by varying the position (one-third from the top, middle, two-third from the top and interface of subgrade and GSB) of geogrid within GSB. The pavement was subjected to repeated load test to simulate traffic loading. The loading frequency was kept at 0.01 Hz. The settlement of the pavement was recorded in terms of total and plastic settlements along the surface below the load point and away from the load point. Based on the test results, the geogrid placed at a depth of two-third thickness of GSB from the top showed improved performance and is effective compared with other positions. With geogrid reinforcement at optimal position, the reduction in plastic settlement is in the order of 34% to 52% depending on the geogrid stiffness and GSB thickness thereby improving the rutting performance of the pavement. Also, with geogrid reinforcement, it is possible to reduce the pavement thickness with equivalent and/or better performance of the pavement when compared to unreinforced pavement depending on the tensile strength of the geogrid. Thus, geogrid can be used to design pavements that are durable and with low maintenance cost making sustainable pavements.

Keywords Pavement · Rutting · Fatigue · Geogrid · Settlement · Service life

Introduction

Geogrid is one among the major forms of geosynthetics which has been used successfully for reinforcing unbound granular materials. Uniaxial, biaxial, and triaxial are the three common types of geogrid. Uniaxial geogrid has rectangular apertures having tensile strength in the longitudinal direction and are commonly used to reinforce slopes, embankments and retaining walls. Biaxial geogrid has square or rectangular apertures having tensile strength in both longitudinal as well as transverse directions. Triaxial geogrid has triangular apertures having tensile strength in all the three directions. Biaxial and triaxial geogrids are used for reinforcing pavements. The geogrid can be used to improve the pavement performance and it is possible to reduce the thickness of pavement resulting in cost reduction [1]. Over the years, several studies have been conducted to study the behavior of geogrid reinforced pavements [2–6], and these studies reported that the geogrid is a viable alternative solution in terms of economy and durability compared to other methods. Geogrid interlocks with aggregate through its apertures. The interlocking between geogrid and aggregate forms a confined zone below and above the geogrid [4, 7–10]. The confinement effect offered by the geogrid increases the modulus of the geogrid reinforced

✉ K. H. Mamatha
mamathakh@sit.ac.in

[1] Department of Civil Engineering, Siddaganga Institute of Technology, Tumkur, Karnataka 572103, India

[2] Department of Civil Engineering, Siddaganga Institute of Technology, Tumkur, Karnataka, India

aggregate layer resulting in improved resistance to vertical stress over the subgrade and consequent reduction in vertical subgrade deformation [4, 10, 11]. The studies showed that the geogrids can extend the service life of a pavement [2, 11–15], reduce base course thickness [13, 16–18] and delay rutting development [15, 19–23]. The improved pavement performance of geogrid reinforced base depends on various factors such as physical properties of geogrid [19–24], mechanical properties of geogrid [5, 13, 15, 21, 25], location of geogrid in pavement [4, 5, 21, 26, 27], subgrade strength [24], thickness of base layer [19, 28], and aggregate base residual stresses [29]. The geogrid improves the subgrade performance through four mechanisms (i.e., separation, confinement, improved load distribution, and tension membrane) which results in reduced stress transfer to the subgrade [21, 23, 24, 26, 30, 31]. Considerable tension membrane effect can be realized when the pavement section is constructed over a weak subgrade (i.e., subgrade with a CBR of less than 3) [30]. The location of geogrid within the base course layer in the pavement system is a crucial factor influencing the effectiveness of reinforcement [5, 27]. Research work in the past have identified the geogrid should be placed near the load, i.e., upper one-third [1, 4, 21, 26], near the bottom, i.e., bottom one-third [3, 32–34], at mid-height [1, 3] and interface of subgrade and base course [2–5, 13, 26, 29, 35, 36]. Ibrahim et al. [37] reported that geogrid placed underneath the asphalt layer greatly reduces the tensile strain at the bottom of asphalt layer. Also, when the geogrid is placed at the interface of subgrade and granular base, the reinforcement reduces the compressive stains at the top of subgrade level but not the tensile strain at the bottom of asphalt layer. As there is no general opinion regarding the optimal position for geogrid placement within a pavement section, there is a need to explore further.

The present study is focused on evaluating the effectiveness of geogrids in pavements and re-examining the optimum location for geogrid placement by carrying out a series of repeated load tests on the model pavement sections. Also, the possibility of reduction in designed pavement thickness is verified through repeated load tests.

Materials

Black cotton soil, crushed aggregate, and silty sand were used for the preparation of model pavement section. The black cotton soil was collected from Bagalkot, Karnataka, India, and used for the preparation of subgrade. Crushed aggregate was collected from a quarry located in Mydala, Tumkur, Karnataka, India, and used in the preparation of sub-base course layer. Silty sand was collected from a local site in Tumkur, Karnataka, India, and used in the preparation of sacrificial layer at the top of model pavement section. The collected materials were tested for their engineering properties, and all the tests were carried out as per the relevant Indian Standards (IS). The properties of the soils used in this study are listed in Table 1. Based on the grain size distribution and plasticity characteristics, the black cotton soil is classified as highly compressible clay with group symbol CH according to IS and unified soil classification systems [38]. It is classified as A-7-C according to HRB classification system and A-7-6 as per AASHTO [39] classification system. Based on the plasticity characteristics, dry unit weight, CBR and swell index, the soil forms a weak subgrade material as per Ministry of Road Transport and Highways, Government of India [40]. Silty sand is classified as well-graded silty sand with group symbol SW-SM according to IS and unified soil classification systems [38]. It is classified as A-2-4 according to HRB and AASHTO [39] classification system. Crushed aggregate was separated into three fractions, i.e., 40 mm down, 12.5 mm down, and stone dust of size 4.75 mm down. The properties of the crushed aggregate along with MoRT&H [40] guidelines are tabulated in Table 2. From the table, it is observed that the aggregate satisfies the strength requirements specified by MoRT&H [40], the three fractions of the crushed aggregate were blended into a mix with different proportions so as achieve the grading II sub-base course material in accordance with IRC: SP: 72 [41]. The designed sub-base mix possesses a maximum

Table 1 Engineering properties of soils

Property	Silty sand	Black cotton soil
Specific gravity	2.66	2.72
Consistency limits (%)		
Liquid limit	28	71
Plastic limit	NP	23
Plasticity index	–	48
Shrinkage limit	18	12
Compaction characteristics		
Modified proctor test		
OMC (%)	9.1	19.4
Maximum dry unit weight (kN/m^3)	19.7	16.8
Standard proctor test		
OMC (%)	13.2	24.2
Maximum dry unit weight (kN/m^3)	18.0	14.6
Unconfined compressive strength (kPa)		
Unsoaked	130	89
Soaked	–	–
California bearing ratio (%)		
Unsoaked condition	7	4
Soaked condition	5	< 2
Swelling index (%)	–	34

Table 2 Properties of crushed aggregate along with MoRT&H [40] guidelines

Test	MoRT&H specifications	Results		Remarks
		40 mm down	12.5 mm down	
Specific gravity	2.5–3.2	2.66	2.64	Good
Aggregate impact value (%)	Max 30%	25	24	Acceptable
Aggregate crushing (%)	Max 30%	22	23	Acceptable
Water absorption (%)	Max 2%	0.4	0.4	Good
Los Angeles abrasion (%)	Max 40%	31	32	Acceptable
Combined indices (%)	Max 30%	27	29	Acceptable

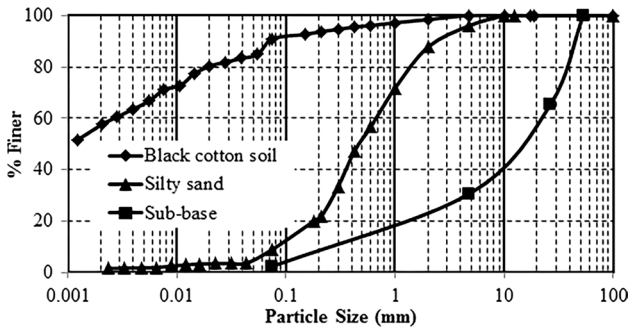

Fig. 1 Particle size distribution curves

Fig. 2 Vibratory compactor

dry unit weight of 21.2 kN/m^3 and optimum water content of 4% under modified proctor condition. Under this condition, the sub-base material showed a CBR of 35% and 30%, under unsoaked and soaked conditions respectively. Figure 1 shows the particle size distribution curves of black cotton soil, silty sand, and crushed aggregate.

Two biaxial geogrids were used to reinforce the model pavement sections and are referred as BX1 and BX2. The geogrids were made up of polyester yarns with square aperture and were procured from Strata Geosystems India Pvt. Ltd., Mumbai. BX1 and BX2 had a tensile strength of 30 kN/m and 40 kN/m, respectively, in both longitudinal and transverse directions. In this study, four locations were identified for the geogrid placement, i.e., one-third from top, middle, two-third from the top of GSB and interface of subgrade and GSB to investigate the effect of position of geogrid on the pavement performance.

Construction of model pavement sections

Stage construction was adopted for the construction of model pavement sections. The test sections were built in a steel tank of size 2 m × 2 m × 2 m. The tank was initially filled with sand up to a depth of 1 m with an average relative density of greater than 85%. The model pavement of size 1 m × 1 m was built using a steel frame of size 1 m × 1 m × 0.3 m. Over the prepared sand deposit, subgrade, sub-base, and sacrificial layers were constructed sequentially. The subgrade and surface layer thicknesses were 300 mm and 50 mm, respectively. Three sub-base course layer thicknesses were considered in the present investigation, i.e., 0.25 m, 0.30 m and 0.35 m in order to study the effect of pavement thickness on the effectiveness of geogrid. The subgrade was compacted manually using a rammer to standard proctor conditions. The sub-base course and sacrificial layers were compacted using vibratory plate compactor to the respective modified proctor conditions. The compactor consists of a base plate of size 0.25 m × 0.25 m and 0.01 m thick. The compactor facilitates compaction at four different frequencies, i.e., 20 Hz, 40 Hz, 60 Hz, and 80 Hz. The vibratory compactor used in this study is shown in Fig. 2. The GSB and sacrificial layers were compacted under a frequency of 80 Hz. In case of geogrid reinforced test sections, the geogrid was placed at the desired location followed by pouring of the material and compaction. All three layers of the model pavement section were compacted in two lifts confirming to MoRT&H [40] guidelines. At the end of compaction of each layer, the density of the compacted layer was determined by suitable methods at a minimum of three points. A relative compaction of greater than 95% for subgrade and 97% sub-base and sacrificial layers was maintained in all the model pavement sections. Figure 3 shows the pictorial view of construction of

model pavement sections. At the end of construction of the test section, the surroundings of the test section were filled with sand which acts as earthen shoulders in pavements. Figures 4 and 5 show the typical pavement section under unreinforced and geogrid reinforced conditions, respectively.

Test setup and procedure

A square steel plate of size 0.30 m x 0.30 m and 0.03m thick was used as test plate to transfer load to the model pavement sections. The size of the loading plate was approximately equal to one-sixth of the width of the test tank, and with this setup, the boundary effects were avoided [42]. On the prepared test section, the test plate was placed exactly at the center of the section. The assembly forms a reaction frame for loading through hydraulic jack of capacity 100 kN with a minimum count of 1 kN. A cylindrical column of 0.135 m diameter and 0.01 m thickness was used as vertical support to transfer the load from the jack to the test plate. A precalibrated proving ring of 200 kN capacity with a minimum count of 0.2 kN was attached between the hydraulic jack and the support to read the applied load. Four dial gauges were mounted one at each corner of the test plate to record the settlement of the test plate. Three dial gauges were mounted along the centerline of the test section on one side of the plate at a distance of 0.83 B, 1.16 B, and 1.5 B from the edge of the plate to record the deformation of the surface. Haversine loading was adopted to simulate the repeated applications of vehicular loading. Initially, the dial gauges were set to zero and the test plate was preloaded to a pressure of 0.7 kg/cm^2 [43]. When no further settlement occurs, the dial gauges were set to zero again. A peak load of

Fig. 3 Pictorial view of construction of model pavement section. **a** compacted subgrade, **b** partially compacted GSB, **c** geogrid with sakes, **d** geogrid layer with overlying GSB material, **e** compacted GSB, **f** compacted sacrificial layer, **g** model pavement section surrounded by sand

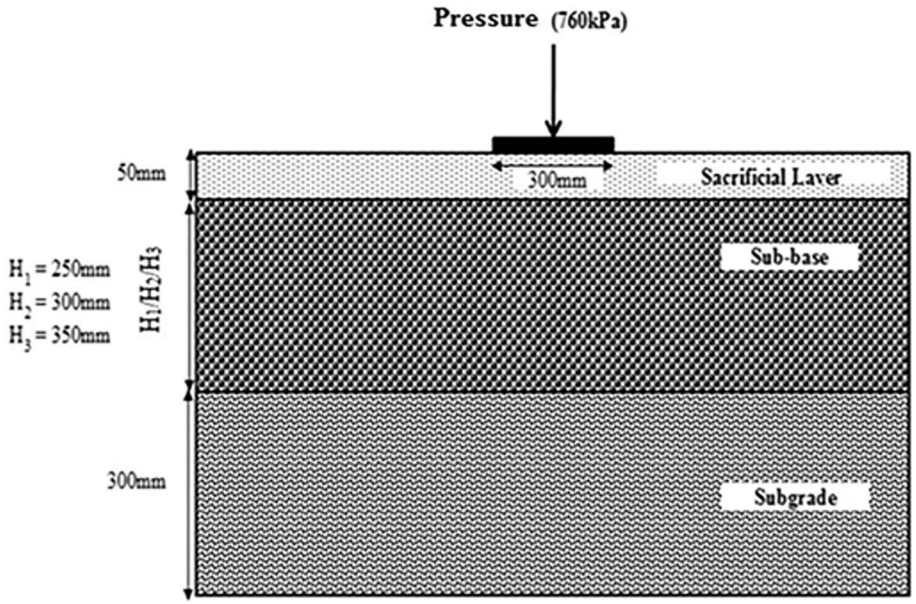

Fig. 4 Typical unreinforced model pavement section

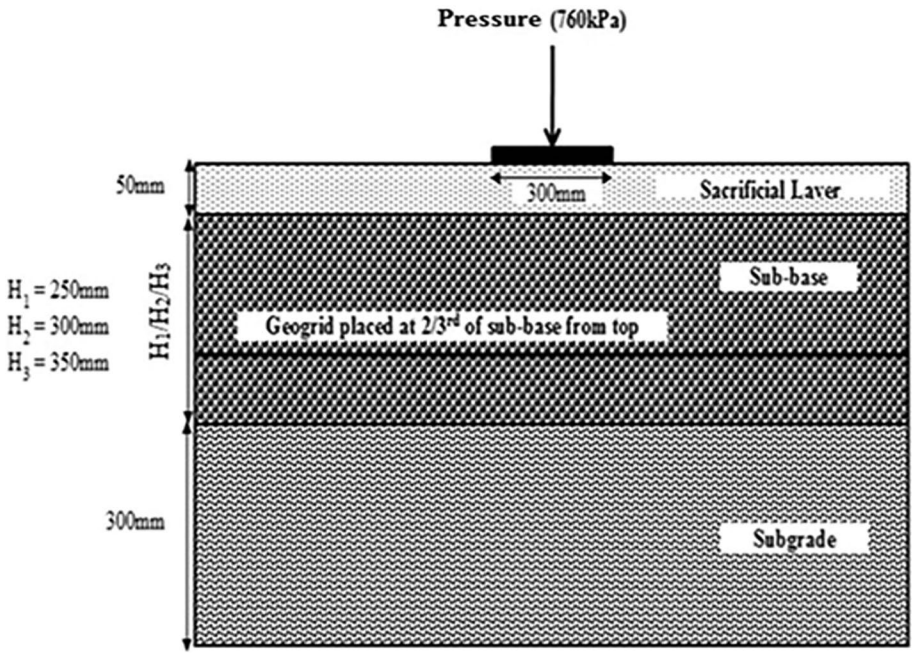

Fig. 5 Typical geogrid reinforced model pavement section

68 kN was considered in order to simulate the tire pressure exerted by a truck with single axle and single wheel on pavements (i.e., 760 kPa). The load was then increased from seating pressure to the peak and unloaded, followed by a rest period. The dial gauge readings were recorded on loading, unloading and at the end of rest period. A total of 500 loading cycles were applied on each test section. At the end of every 10 loading cycles, the dial gauge readings were recorded. Figure 6 shows the experimental setup.

Results and discussions

A series of repeated load tests were carried out on unreinforced and geogrid reinforced model pavement sections. The effect of provision of geogrid within the pavement structure on the pavement performance was investigated. The influence of tensile strength of geogrid and its position and the thickness of granular layer on the pavement performance was studied. The deformation characteristics of the model pavements under repetitive loading and the influence

Fig. 6 Experimental setup for repeated load test

of geogrid and their properties on the performance of the model pavements are presented and discussed in the following paragraphs.

Figures 7a–c, 8a–c, and 9a–c show the variation of total, plastic, and elastic settlement with the number of load cycles of unreinforced and geogrid reinforced (with varied geogrid position) model pavement sections with sub-base thicknesses of (a) 0.25 m, (b) 0.30 m and (c) 0.35 m, respectively. In both unreinforced and geogrid reinforced pavement sections, plastic settlement accounts for 86% to 92% of the total settlement and elastic settlement accounts for about 8% to 14% of the total settlement. This clearly indicates the predominant rutting behavior of pavements. It is observed that the total and plastic settlements increased with increase in the number of load cycles in the unreinforced model pavement section. The total and plastic settlements of geogrid reinforced test sections follow the same trend as in case of unreinforced test section with the reduced magnitude depending on the stiffness of geogrid and its position. Also, the pavement section with thicker sub-base course layer showed lesser settlement irrespective of the test condition and this is attributed to the increased durability of the thicker layer. At 50 load cycles which correspond to a traffic volume of 50CVPD (commercial vehicles per day), about 45% to 73% of the total settlement and plastic settlements occur in both unreinforced and geogrid reinforced (with varied geogrid stiffness, position and sub-base thickness) test sections when compared with the respective total and plastic settlements at the end of 500 load cycles which correspond to a traffic volume of 500CVPD. The geogrid reinforcement does not show any significant influence on the elastic behavior of the test section, and the elastic settlement remains almost same irrespective of the test condition.

The provision of geogrid provides resistance to lateral movement of aggregates in the granular sub-base and the degree of resistance depends on the properties of geogrid such as stiffness of geogrid and its position. Increased geogrid stiffness results in improved performance for all pavement thicknesses and positions of geogrid. The position of geogrid is found to have a significant influence on the pavement performance. When the geogrid is placed near to the top surface (i.e., at one-third of sub-base from its top surface), the geogrid was subjected to compression under the application of repetitive loading and the tension stress developed at the interface of geogrid and sub-base course material is very less leading to an insignificant reduction in the settlement. In this position of geogrid, the reduced settlement is due to the particle interlocking mechanism. When the position of geogrid is shifted downwards (i.e., mid-height of sub-base), the geogrid is still subjected to compression and the lateral stresses developed are higher than that of one-third position leading to an increased reduction in the settlement. The improved performance is attributed to particle interlocking and partial tension membrane effect. When the geogrid is placed at two-third of sub-base thickness from its top surface, the tensile stresses developed at the interface of geogrid and the sub-base course material are higher and therefore, the degree of resistance offered by the geogrid against lateral flow is maximum at this location. The maximum reduction in the settlement at this location is attributed to both particle interlocking and tension membrane effect. When the geogrid is shifted further downwards (i.e., at the interface of subgrade and sub-base), the geogrid offers resistance to deformation but it is found to be lesser when compared with that of two-third position. This is due to the reduced particle interlocking and reduced interface friction due to the presence of friction material on the top and cohesive material at the bottom. Based on the above discussions, it is concluded that the geogrid placed at two-third of sub-base thickness from the top (i.e., two-third) yields maximum reduction in settlement and improved pavement performance in terms of rutting.

To compare the effectiveness of geogrid reinforcement numerically, a parameter called reduction in plastic or permanent settlement (RPS) is used [1, 44]. RPS is defined as a ratio of difference between permanent settlement of

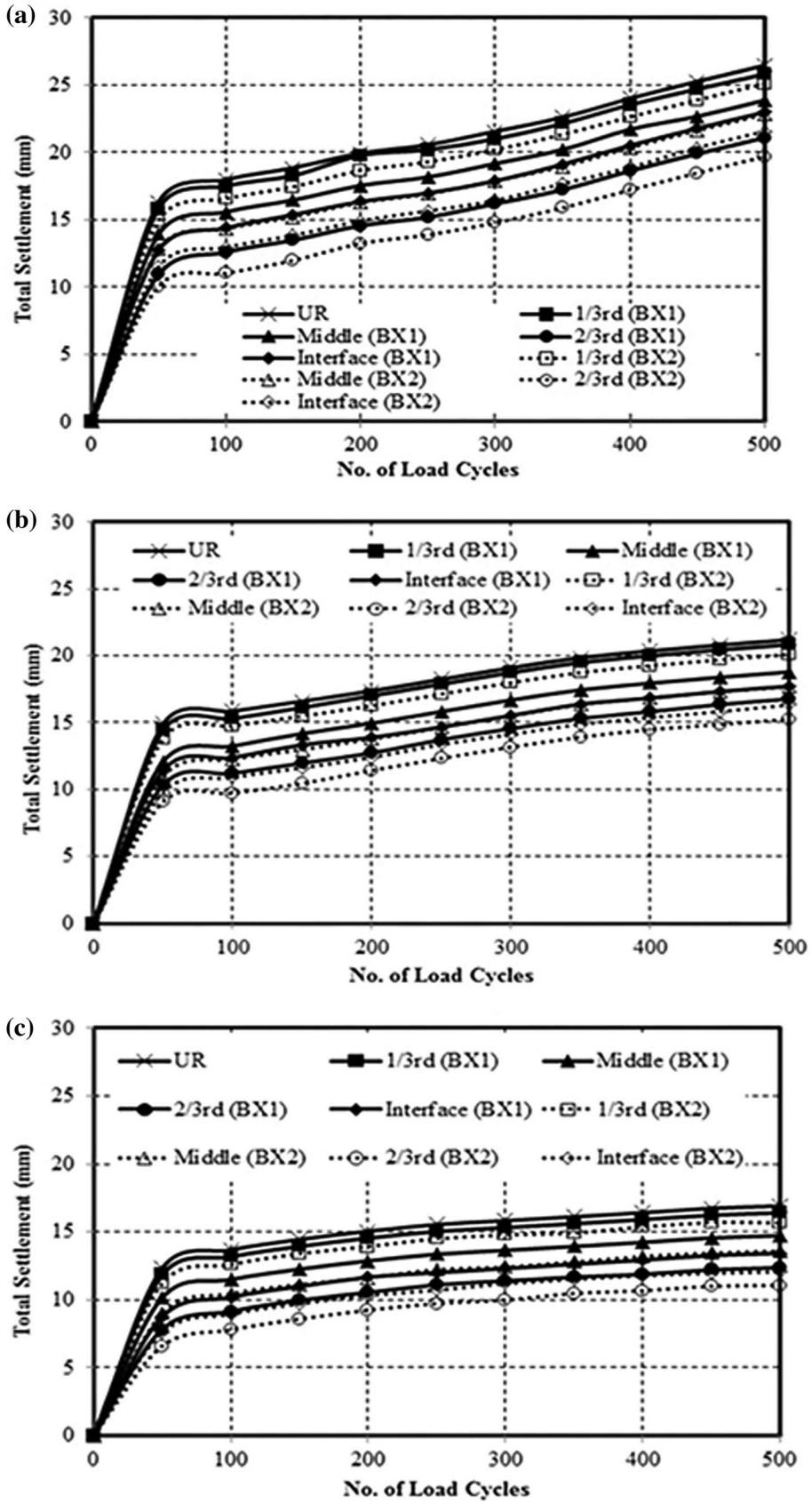

Fig. 7 Total settlement versus the number of load cycles of unreinforced and geogrid reinforced model pavement sections with GSB of thickness **a** 0.25 m, **b** 0.30 m, **c** 0.35 m

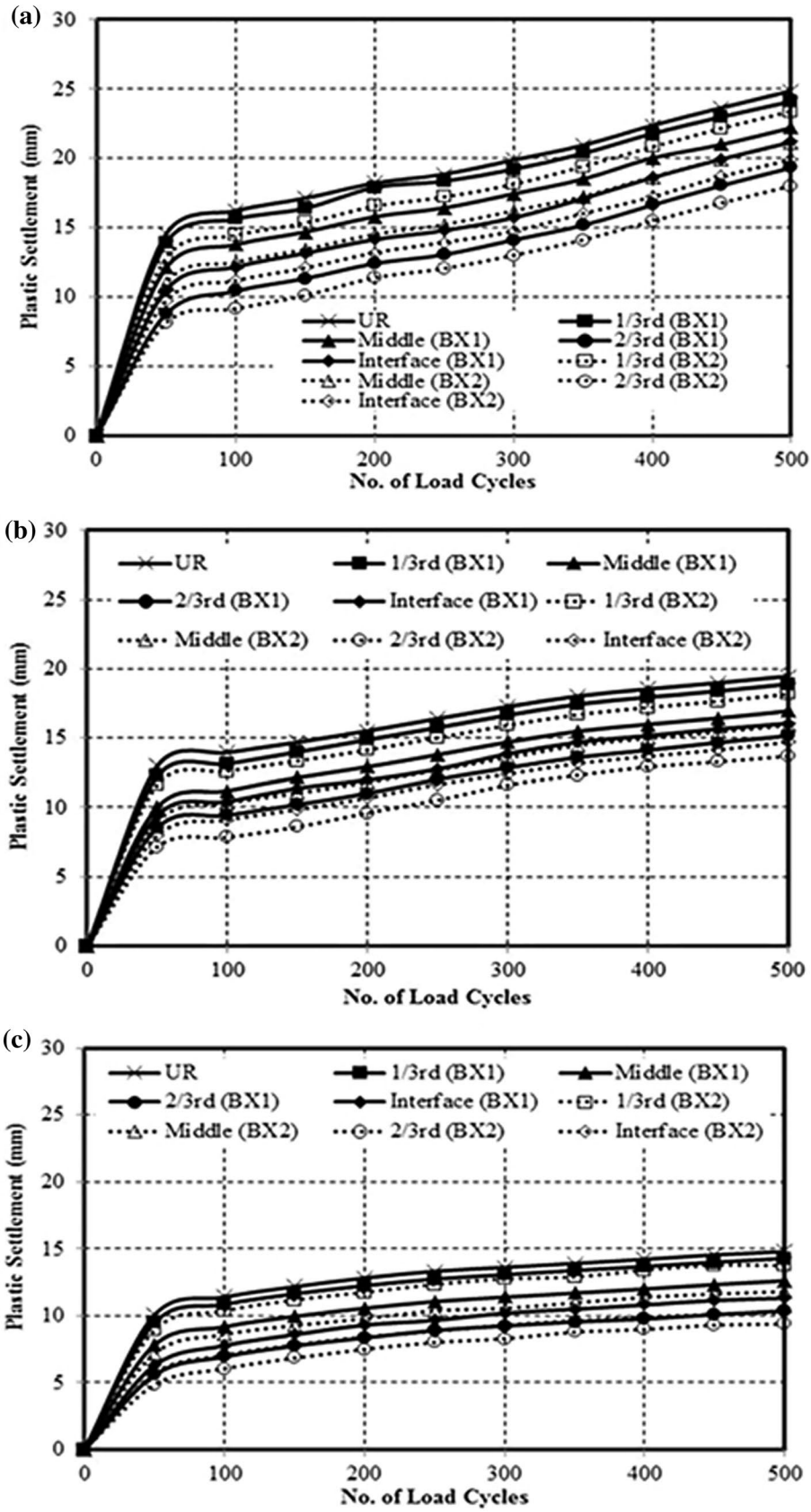

Fig. 8 Plastic settlement versus the number of load cycles of unreinforced and geogrid reinforced model pavement sections with GSB of thickness **a** 0.25 m, **b** 0.30 m, **c** 0.35 m

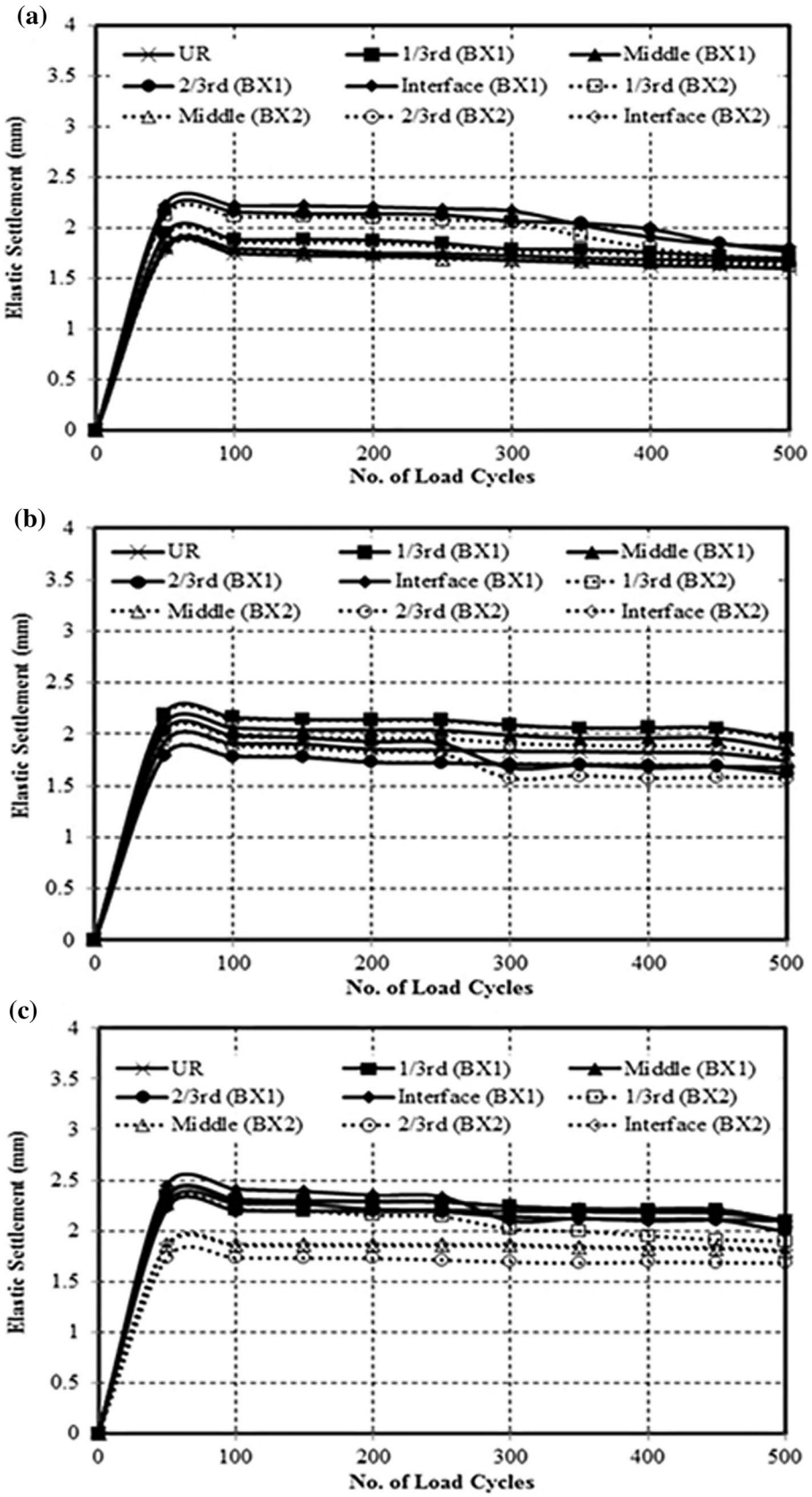

Fig. 9 Elastic settlement versus the number of load cycles of unreinforced and geogrid reinforced model pavement sections with GSB of thickness **a** 0.25 m, **b** 0.30 m, **c** 0.35 m

unreinforced pavement section and permanent settlement of geogrid reinforced pavement section to permanent settlement of unreinforced pavement section with the number of load cycles being constant. It is expressed in terms of percentage and is given by Eq. (1).

$$\mathrm{RPS} = \frac{P_{\mathrm{UR}} - P_{\mathrm{RE}}}{P_{\mathrm{UR}}} \times 100 \quad (1)$$

where RPS = percentage reduction in plastic/permanent settlement, P_{UR} = permanent settlement of unreinforced pavement section at the end of N number of load cycles, P_{RE} = permanent deformation of geogrid reinforced pavement section at the end of N number of load cycles.

Figure 10a–c shows the variation of reduction in plastic settlement (RPS) with the number of load cycles of geogrid reinforced pavement sections with sub-bases of thickness (a) 0.25 m, (b) 0.30 m, and (C) 0.35 m, respectively. For the model pavement section with 0.25 m sub-base thickness, geogrid reinforcement positioned at one-third of sub-base from its top surface was found to perform similar to that of and/or slightly better than the respective unreinforced pavement section and did not show any appreciable increase in the RPS values irrespective of the geogrid stiffness. Reinforcing the geogrid at mid-height of sub-base resulted in increased RPS values when compared with that of the pavement section reinforced at one-third the height of sub-base from its top surface. The pavement section with geogrid reinforcement at two-third of sub-base from its top surface showed increased RPS values when compared with that of the pavement section reinforced with geogrid at one-third and mid-height of sub-base from its top surface and this position is the optimum location. When the geogrid is placed in the tension zone (i.e., near to the bottom), the geogrid layer develops tensile stresses at the interface of sub-base and geogrid due to lateral flow of granular layer resulting in the development of tension membrane effect yielding higher RPS values. At the interface of subgrade and sub-base, though the geogrid layer develops tension membrane effect yields lower RPS values when compared with that of two-third of sub-base from its top. The reduced RPS value is attributed to the particle interlocking mechanism. When the geogrid is placed within the sub-base (i.e., at two-third of sub-base from its top), the aggregate particles present above and below the geogrid forms a stiffer zone when compared to the geogrid placed at the interface where the aggregate particles present above the geogrid and soil below the geogrid. At the interface, non-homogeneous materials at the top and bottom result in unequal friction mobilization. Similar observations were found for pavement sections with a sub-base of 0.30 m and 0.35 m thick. At 50 load cycles (i.e., 50CVPD), the highest benefit (RPS) generated by the geogrid BX1 is 5% to 6%, 17% to 23%, 34% to 40% and 28% to 37%, respectively, when the geogrid is positioned at one-third, middle, two-third of sub-base from its top and interface of subgrade and sub-base with varied sub-base thicknesses. Similarly, the highest benefit (RPS) offered by the geogrid BX2 is 10% to 12%, 24% to 31%, 44% to 52% and 33% to 43%, respectively, when the geogrid is positioned at one-third, middle, two-third of sub-base from its top and interface of subgrade and sub-base with varied sub-base thicknesses. At the end of 500 load cycles (i.e., 500CVPD), the RPS values were found to be reduced and this is attributed to the degradation of aggregate particles. The reduced RPS value ranges from 3 to 37% at the end of 500 load cycles with varied geogrid stiffness, its position and sub-base thickness.

Figure 11a–c shows the surface profiles of total settlement of unreinforced and geogrid reinforced model pavement sections with sub-base of thickness (a) 0.25 m, (b) 0.30 m and (c) 0.35 m at the end of 50 and 500 load cycles. The number of load cycles is given in the parenthesis. It is observed that the increased number of load cycles showed increased heaving at the edge of the loading plate. However, thicker pavement section showed lesser heaving. The surface heaving was found to be reduced with the provision of geogrid irrespective of the geogrid stiffness and sub-base thickness. The geogrid reinforced at two-third of sub-base from its top showed minimum heave at the surface when compared with the other positions considered irrespective of the stiffness of geogrid and sub-base thickness. This is attributed to the tension membrane effect and particle interlocking mechanism. At a particular geogrid position, BX2 was found to be effective in reducing the surface heave when compared with BX1 which indicates the effect of geogrid stiffness in minimizing surface heave and consequently reduced rutting.

As per IRC: 115 [45], rut depth is defined as the maximum perpendicular distance measured between the bottom surface of a 3 m straight edge and the contact area of the gauge with the pavement surface at a specific location and the rut depth was determined from the test results. Figure 12 shows the schematic representation of rut depth as per IRC: 115 [45]. IRC: SP: 20 [46] specifies a maximum permissible rut depth of 50 mm for unpaved roads or gravel roads. If a pavement structure develops a rut depth beyond the maximum permissible limit, the pavement is considered unserviceable and necessary maintenance or rehabilitation must be resorted to (2014).

Figure 13a–c shows the variation of rut depth with the number of load cycles of unreinforced and geogrid reinforced (at two-third of sub-base from its top) pavement sections with sub-bases of thickness (a) 0.25 m, (b) 0.30 m and (c) 0.35 m. The unreinforced test section develops significant rut depths with 50 load cycles (i.e., 50CVPD) and it further increased significantly with the increased load cycles

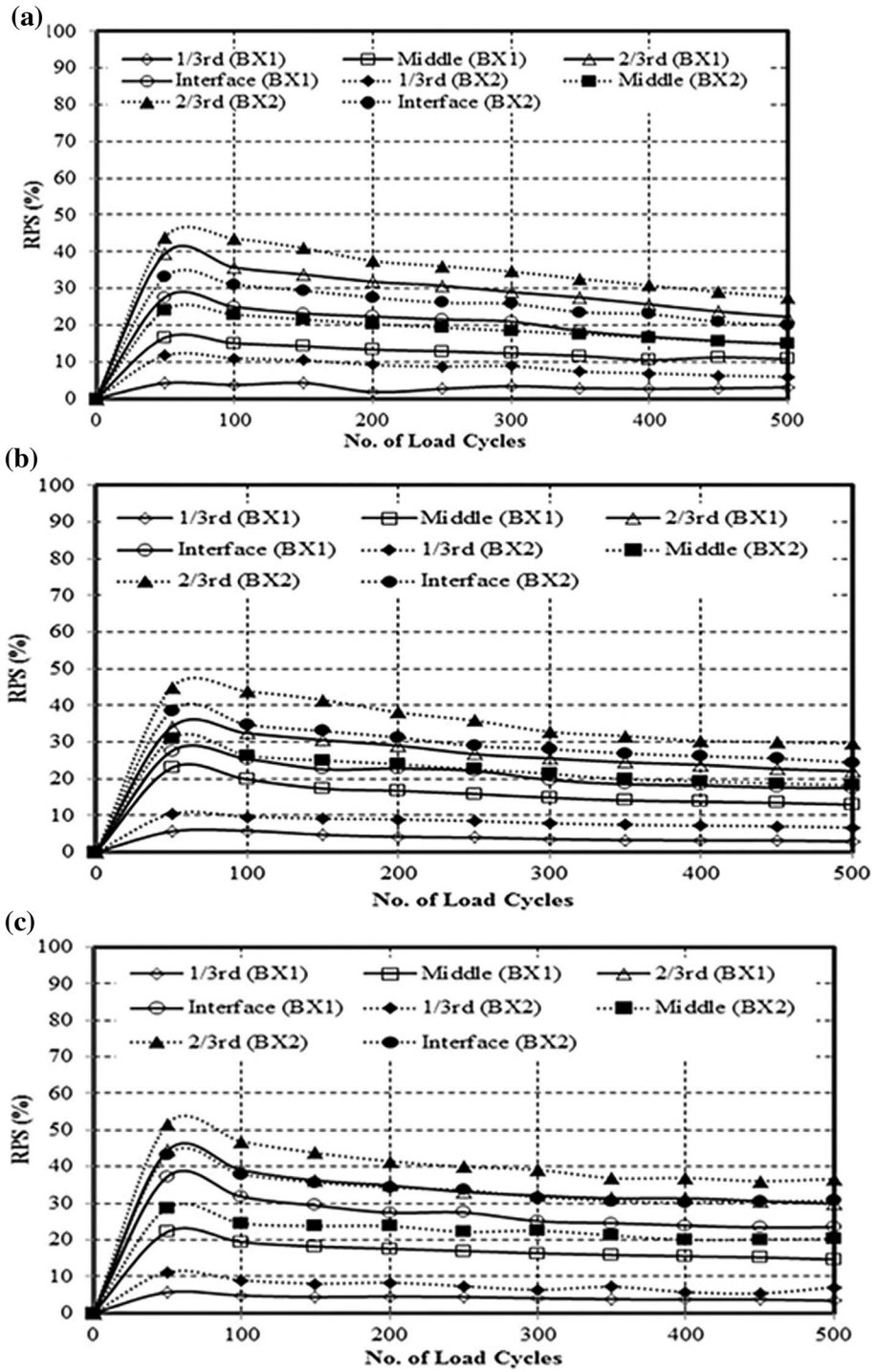

Fig. 10 Reduction in plastic settlement (RPS) versus the number of load cycles of geogrid reinforced pavement sections with GSB of thickness of **a** 0.25 m, **b** 0.30 m, **c** 0.35 m

irrespective of the sub-base thickness. The geogrid reinforced test sections follow a similar trend with the reduced rut depths. At 50 load cycles (i.e., 50CVPD), the measured rut depths are 12 mm to 18 mm, 7 mm to 11 mm, and 6 mm to 11 mm, respectively, in the case of unreinforced, BX1 and BX2 reinforced test sections with sub-base thickness ranging from 0.25 to 0.35 m. At 500 load cycles (i.e., 500CVPD), the measured rut depths are 19 mm to 33 mm, 14 mm to 25 mm and 12 mm to 23 mm, respectively, in the case of unreinforced, BX1 and BX2 reinforced test sections with sub-base thickness ranging from 0.25 to 0.35 m. Between 50 to 500 load cycles, the increase in rut depth is 7 mm to 15 mm in unreinforced section and 6 mm to 14 mm in BX1 reinforced section and 6 mm to 12 mm in BX2 reinforced test section with sub-base thickness ranging from 0.25 to 0.35 m. Among the two geogrids considered, BX2 is better

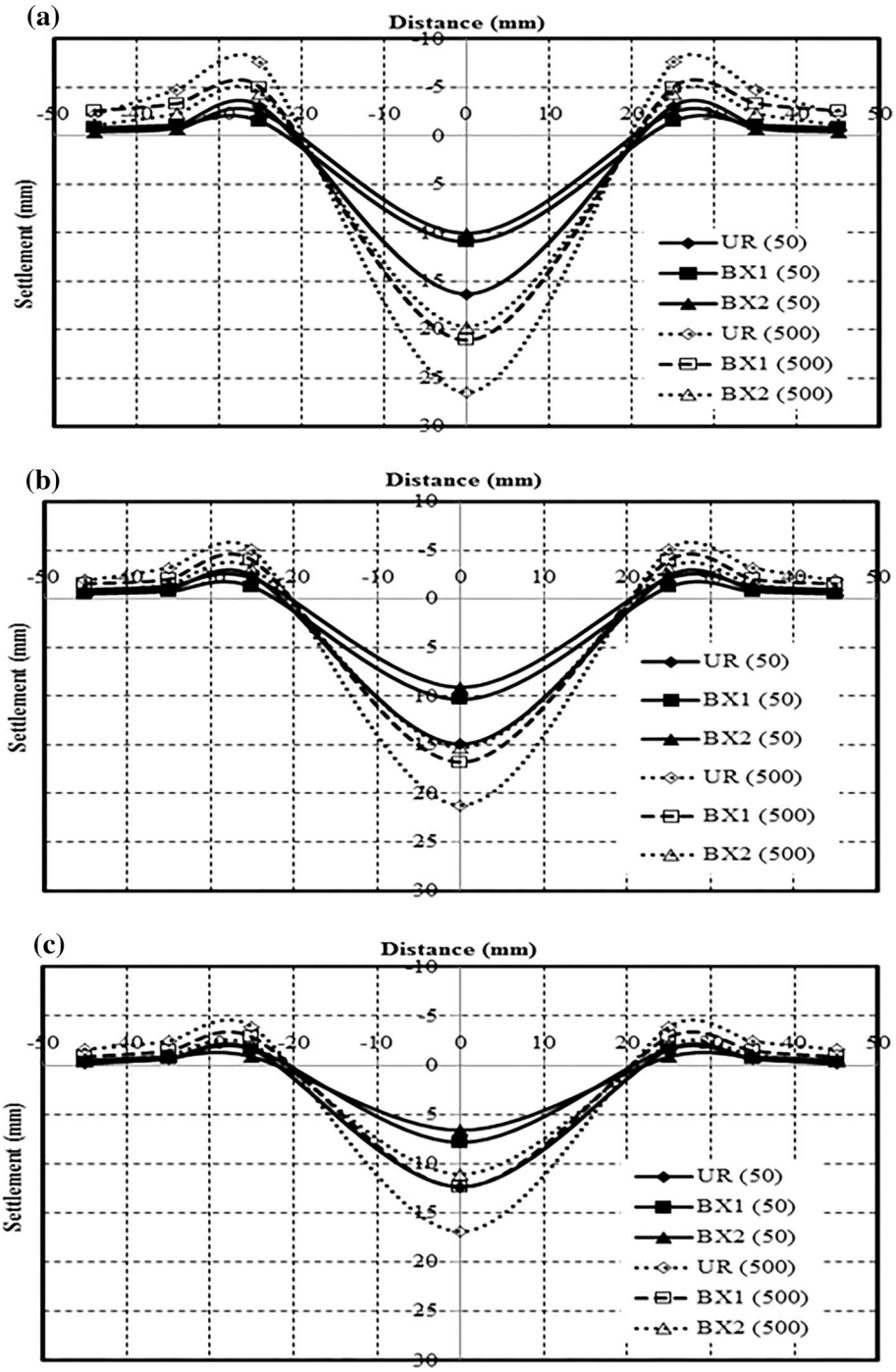

Fig. 11 Surface profiles of settlement of unreinforced and geogrid reinforced (at two-third of GSB from its top surface) pavement sections with GSB of thickness **a** 0.25 m, **b** 0.30 m, **c** 0.35 m at the end of 50 and 500 load cycles

in improving the serviceability conditions of roads over a longer duration, and thereby, the sustainability of the pavement improves.

As the tests were terminated at 500 load cycles, the rut depth accumulation was forecasted by considering the pattern of increase in rut depth with the number of load cycles. Figure 14a–c shows the variation of forecasted rut depth with the number of cycles for unreinforced and geogrid reinforced (at two-third of sub-base from its top) pavement sections with sub-base of thicknesses (a) 0.25 m, (b) 0.30 m and (c) 0.35 m. From the figure it is observed that the unreinforced model pavement sections with sub-base of 0.25 m, 0.30 m and 0.35 m thicknesses are serviceable up to 1000, 1550 and 2250 load cycles, respectively and at this stage the rut depth reaches a value of 50 mm which is the maximum permissible rut depth for unsurfaced roads as per IRC: SP: 72 [41]. The pavement section reinforced with BX1 and BX2 reinforced at two-third of sub-base from its top were

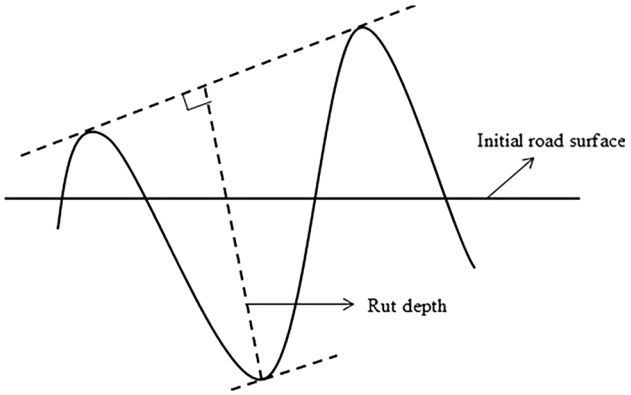

Fig. 12 Schematic representation of rut depth as per IRC: 115 [45]

found to be serviceable up to 1300 and 1450 load cycles, 1800 and 2150 load cycles and 3300 and 3500 load cycles, respectively, for sections with sub-base of thickness 0.25 m, 0.30 m and 0.35 m, respectively. Based on this forecast, with BX1 and BX2 the serviceability of the pavement section is found to increase by 1.2 to 1.5 times and 1.4 to 1.6 times for the sub-base thicknesses considered. Thus, the provision of geogrid within the pavement structure increases the service life of the pavements and the degree of improvement depends on the geogrid position and stiffness of geogrid.

Two non-dimensional parameters called improvement factor [42, 44] and traffic benefit ratio [44, 47–50] are used to quantify the benefit of geogrid reinforcement. Improvement factor (I_f) is defined as the ratio of plastic settlement in unreinforced pavement section to the plastic settlement in geogrid reinforced pavement section with the load cycles being constant and is given by Eq. 2. Traffic benefit ratio (TBR) is defined as a ratio of the number of load cycles in geogrid reinforced pavement section to the number of load cycles in unreinforced pavement section to obtain a constant permanent settlement and is given by Eq. 3.

$$I_f = \frac{P_{UR}}{P_{RE}} \tag{2}$$

where, I_f = improvement factor, P_{UR} = plastic settlement in unreinforced pavement section at the end of N load cycles, P_{RE} = plastic settlement in geogrid reinforced pavement section at the end of N load cycles.

$$\text{TBR} = \frac{N_{RE}}{N_{UR}} \tag{3}$$

where, TBR = traffic benefit ratio, N_{UR} = number of load cycles in unreinforced pavement section corresponding to 'X' settlement, N_{RE} = number of load cycles in geogrid reinforced pavement section corresponding to 'X' settlement.

Figures 15a–b and 16a–b show the variation of improvement factor (I_f) and traffic benefit ratio (TBR) of geogrid reinforced pavement sections with thickness of sub-base for BX1 and BX2, respectively. It is observed that the maximum I_f and TBR values were observed for the pavement sections reinforced with geogrid placed at two-third of sub-base from its top surface. This once again confirms that the location for optimum position of geogrid placement within the pavement structure is two-third of the thickness of granular layer from its top surface. The I_f and TBR are approximately 1 for pavements with geogrid placed at one-third of sub-base from its top surface. The values of I_f and TBR increases in the order of middle of sub-base, interface of subgrade and sub-base and two-third of sub-base from its top surface. It is observed that higher the stiffness of geogrid, the corresponding values of I_f and TBR will be maximum. With BX1 and BX2 (positioned at two-third of sub-base from its top), the maximum I_f values are in the order of 1.50 to 1.79, 1.52 to 1.81 and 1.80 to 2.07, respectively, for pavement sections with sub-base thicknesses of 0.25 m, 0.30 m and 0.35 m, respectively. Similarly, with BX1 and BX2 (positioned at two-third of sub-base from its top), the maximum TBR values are in the order of 1.57 to 1.89, 1.60 to 1.9 and 1.85 to 2.15, respectively, for pavement sections with 0.25 m, 0.30 m and 0.35 m thick sub-base.

Table 3 shows the summary of repeated load tests carried out on unreinforced and geogrid reinforced model pavement sections with varying sub-base thickness, geogrid stiffness, and geogrid position. It is observed that with the provision of geogrid at the optimal position it is possible to optimize the pavement thickness by 50 mm with equivalent/slightly better performance of that of unreinforced section depending on the geogrid stiffness.

Conclusions

A laboratory study was carried out on model pavement sections built in a steel tank with unreinforced and geogrid reinforced conditions to evaluate the effectiveness of geogrid, its stiffness, and position on the pavement performance by carrying out repeated load tests. Based on the test results, the following conclusions are drawn.

- The provision of geogrid within the pavement section, its stiffness, and position influence the pavement performance significantly. Providing the geogrid reinforcement at two-third of the thickness of granular layer from the top is very effective in improving the pavement performance and is attributed to tension membrane effect and particle interlocking mechanism. Higher the geogrid stiffness, better will be the pavement performance.

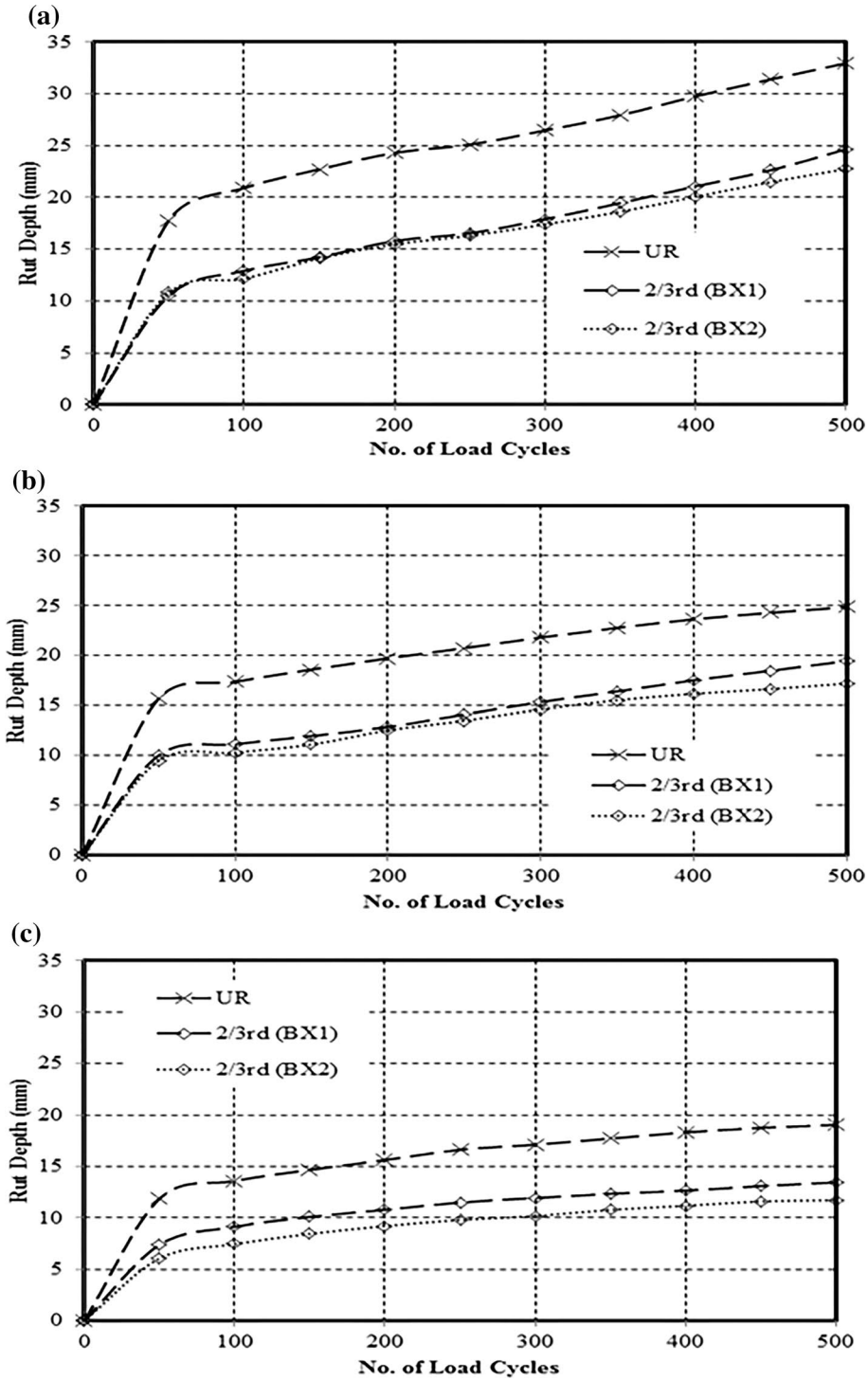

Fig. 13 Rut depth versus the number of load cycles of unreinforced and geogrid reinforced (at two-third of GSB from its top) pavement sections with GSB of thickness **a** 0.25 m, **b** 0.30 m, **c** 0.35 m

- The provision of geogrid at optimal position reduced the plastic settlement significantly and therefore leads to improved rutting behavior. The reduction in plastic settlement is in the order of 34% to 52% depending on the geogrid stiffness and granular layer thickness. The rut life of the pavement is found to increase by 1.2 to 1.6 depending on the geogrid stiffness and granular layer thickness. However, the geogrid reinforcement has no significant effect on the elastic behavior of pavements.
- The provision of geogrid reduced the heaving at the edges of the pavement compared to unreinforced pavement section and this reduction increased with increase in geogrid stiffness thus improving the riding quality and providing comfort to the road users.

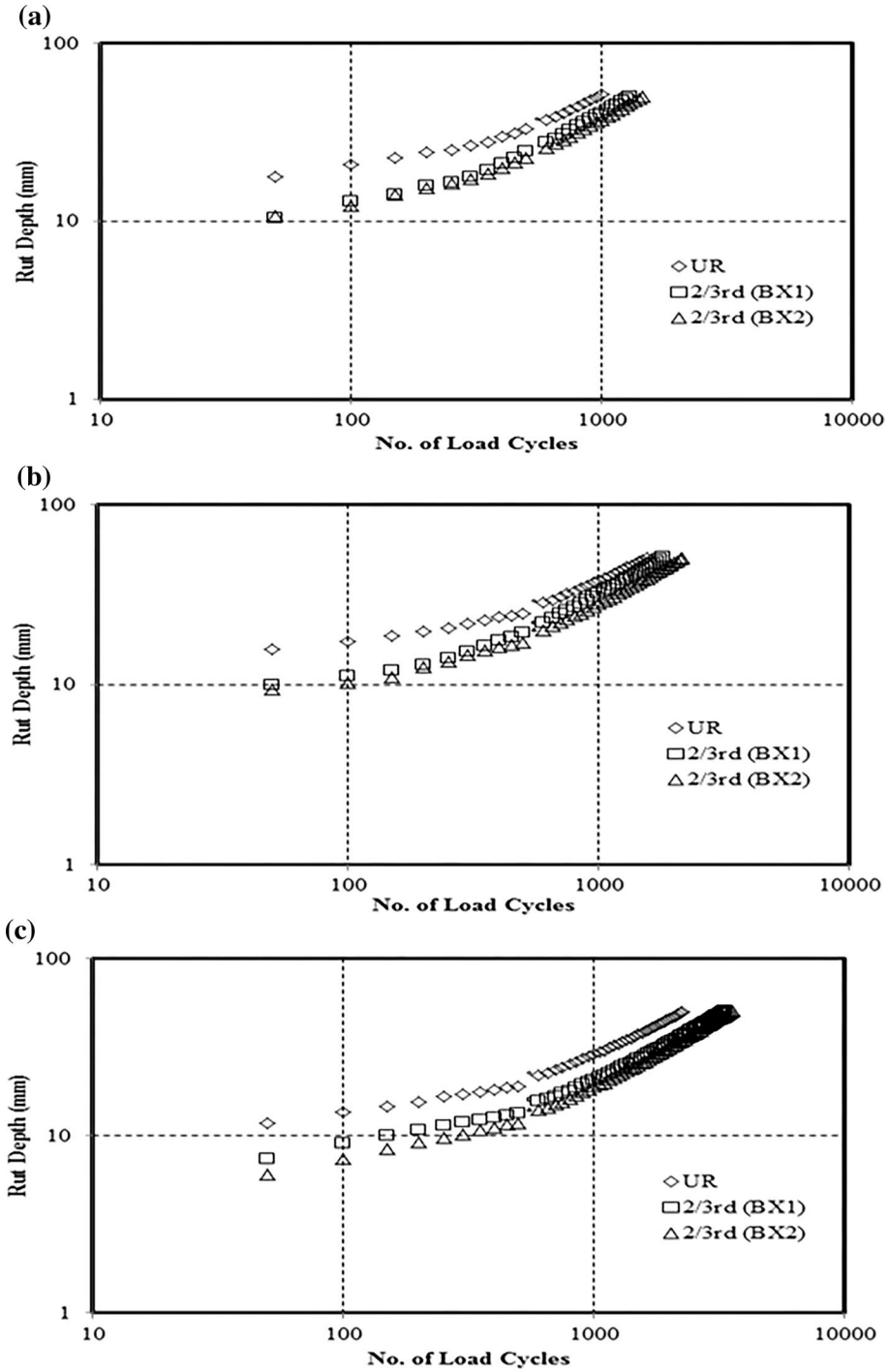

Fig. 14 Forecast rut depth versus the number of load cycles of unreinforced and geogrid reinforced (at two-third of GSB from its top) pavement sections with GSB of thickness **a** 0.25 m, **b** 0.30 m, **c** 0.35 m

- The improvement factor and traffic benefit ratio were found in the range of 1.50 to 2.07 and 1.57 to 2.15 for varied geogrid stiffness and granular layer thickness.
- With geogrid reinforcement, it is possible to reduce the thickness of the pavement by 50 mm with equivalent and/or slightly better pavement performance when compared to unreinforced pavement section.
- However, further studies on the performance of geogrid reinforced sections using accelerated load teats and intelligent sensors are necessary.

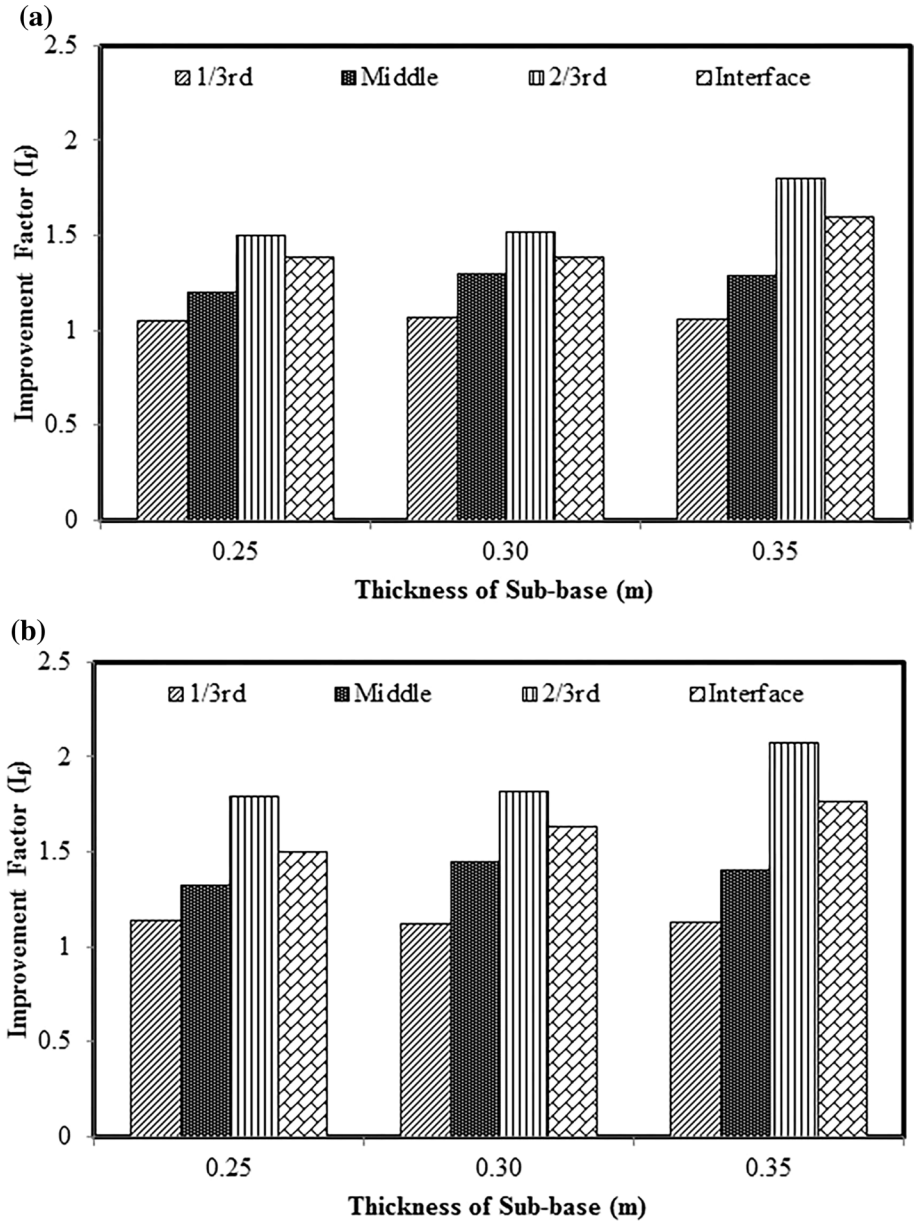

Fig. 15 Variation of improvement factor of geogrid reinforced (a) BX1 (b) BX2 pavement sections with thickness of GSB

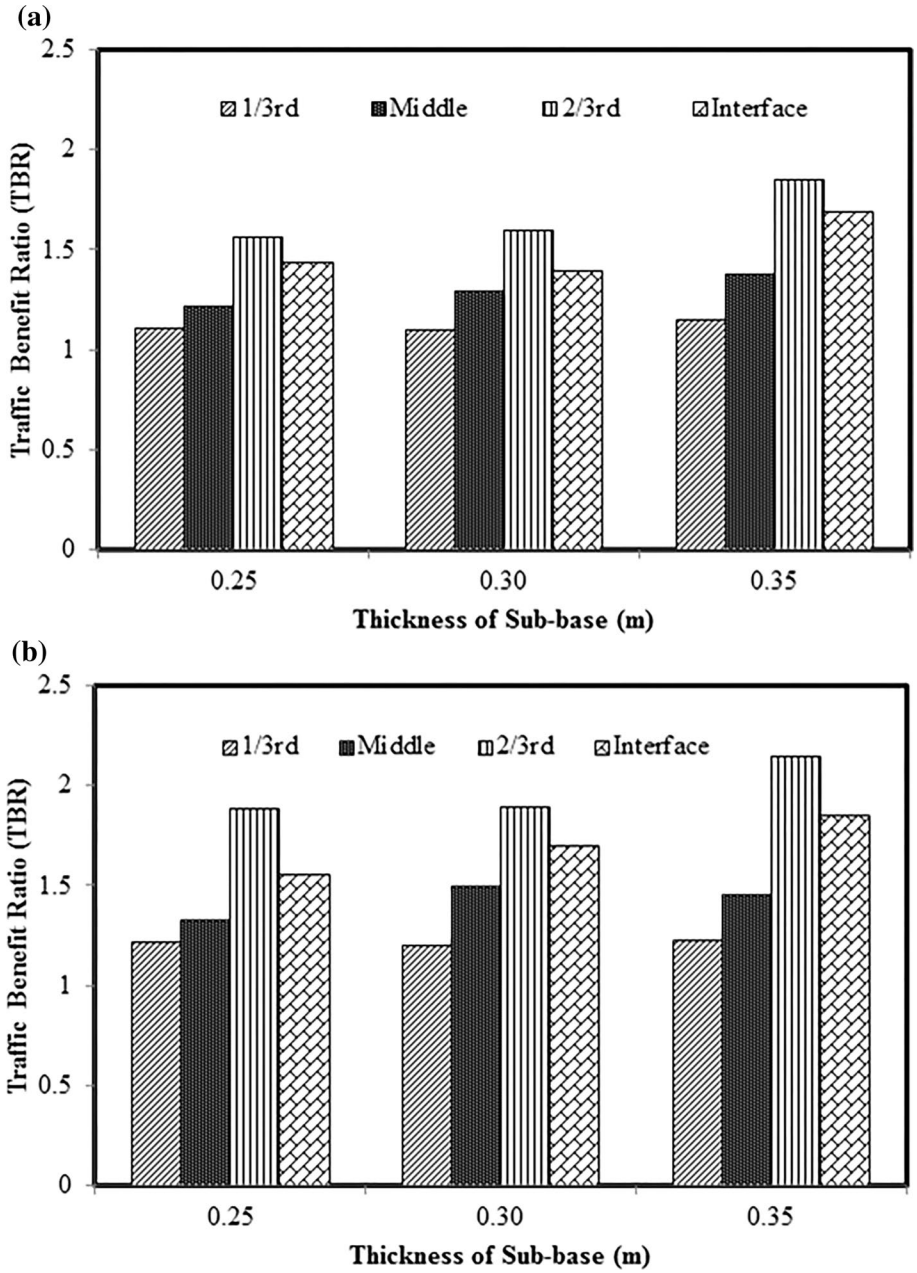

Fig. 16 Variation of traffic benefit ratio of geogrid reinforced **a** BX1, **b** BX2 pavement sections with thickness of GSB

Table 3 Repeated load test results (total and plastic settlement) of unreinforced and geogrid reinforced model pavement sections with varying sub-base thickness, geogrid stiffness, and geogrid position

Total settlement (mm)							% Reduction			
Type of geogrid	GSB thickness (m)	Position of geogrid from the top of sub-base								
		UR	One-third	Middle	Two-third	Interface	One-third	Middle	Two-third	Interface
BX_1	0.25	26.5	25.8	23.9	21.1	22.9	2.5	9.8	20.3	13.2
	0.30	*21.2*	20.9	18.8	16.8	17.7	1.7	11.4	20.9	16.4
	0.35	16.9	16.4	14.7	12.4	13.4	2.9	12.9	26.8	20.6
BX_2	0.25	26.5	25.1	22.8	19.7	21.6	5.2	13.8	25.7	18.6
	0.30	21.2	20.1	17.7	15.3	16.3	5.2	16.7	28.0	22.9
	0.35	16.9	15.7	13.6	11.1	12.1	7.4	19.5	34.6	28.7
Plastic settlement (mm)							% Reduction			
Type of geogrid	GSB thickness (mm)	Position of geogrid from the top of sub-base								
		UR	One-third	Middle	Two-third	Interface	One-third	Middle	Two-third	Interface
BX_1	0.25	24.9	24.2	22.2	19.3	21.2	3.0	10.7	22.3	14.9
	0.30	19.5	18.9	16.9	15.2	16.1	2.9	12.9	22.1	17.5
	0.35	14.8	14.3	12.6	10.4	11.3	3.4	14.7	29.9	23.5
BX_2	0.25	24.9	23.4	21.2	18.0	19.9	5.9	14.9	27.6	19.9
	0.30	19.5	18.2	15.9	13.7	14.7	6.7	18.3	29.7	24.4
	0.35	14.8	13.8	11.8	9.4	10.3	7.1	20.2	36.6	30.7

Acknowledgements The authors acknowledge Prof. T G Sitharam and Department of Civil Engineering, Indian Institute of Science, Bangalore for providing the steel tank free of cost to the Department of Civil engineering, Siddaganga Institute of Technology, Tumkur, for the research work. The authors also acknowledge STRATA Geosystems India Pvt. Ltd. for providing the geogrid samples free of cost to carry out this work.

Compliance with ethical standards

Conflict of interest No potential conflict of interest was reported by the authors.

References

1. Abu-Farsakh M, Souci G, Voyiadjis GZ, Chen Q (2012) Evaluation of factors affecting the performance of geogrid reinforced granular base material using repeated load triaxial tests. J Mater Civ Eng 24(1):72–83
2. Al-Qadi IL, Brandon TL, Valentine RJ, Smith TE (1994) Laboratory evaluation of geosynthetic reinforced pavement sections. Transportation research record, 1439, Transportation Research Board, National Research Council, Washington, DC, pp 25–31
3. Barksdale RD, Brown SF, Chan F (1989) Potential benefits of geosynthetics in flexible pavement systems. National co-operative highway research program report no. 315, Transportation Research Board, National Research Council, Washington, DC
4. Hass R, Walls J, Carroll RG (1988) Geogrid reinforcement of granular bases in flexible pavements. Transportation Research Record, 1188, Transportation Research Board, National Research Council, Washington, DC, pp 19–27
5. Perkins SW (1999) Mechanical response of geosynthetic reinforced flexible pavements. Geosynth Int 6(5):347–382
6. Perkins SW (2002) Evaluation of geosynthetic reinforced flexible pavement systems using two pavements test facilities. Report no. FHWA/MT-02-008/20040, Montana Department of Transportation, Helena, MT
7. Brown SF, Kwan J, Thom NH (2007) Identifying the key parameters that influence geogrid reinforcement of railway ballast. Geotext Geomembr 25(6):326–335
8. Giroud JP, Han J (2004) Design method for geogrid reinforced unpaved roads. I. Development of design method. J Geotech Geoenviron Eng 130(8):775–786
9. Giroud JP, Han J (2004) Design method for geogrid reinforced unpaved roads. II. Calibration and applications. J Geotech Geoenviron Eng 130(8):787–797
10. Love (1984) Model testing of geogrids in unpaved roads. University of Oxford, Oxford
11. Mamatha KH, Dinesh SV, Dattatreya JK (2018) Evaluation of flexural behaviour of geosynthetic-reinforced unbound granular material beams. Road Materials and Pavement Design 20 (4):859-876
12. Al-Qadi IL, Brandon TL, Bhutta SA (1997) Geosynthetic stabilized flexible pavements. In: Proceedings of conference on geosynthetics. Industrial Fabrics Association International (IFAI), Roseville, MN, pp 647–661
13. Cancelli A, Montanelli F (1999) In-ground test for geosynthetic reinforced flexible paved roads. In: Proceedings of conference on geosynthetics. Industrial Fabrics Association International (IFAI), Roseville, MN, pp 863–878
14. Wasage TLJ (2004) Laboratory evaluation of rutting resistance of geosynthetics reinforced asphalt pavement. J Inst Eng Singap 44(2):29–44

15. Mamatha KH, Dinesh SV, Swamy BC (2018). Performance of geosynthetic reinforced model pavements under repetitive loading. Geotech Eng J of the SEAGS & AGSSEA, 49 (4).
16. Iniyan K (2012) Influence of geogrid reinforcement on the carbon footprint of flexible pavements. Thesis submitted in partial fulfillment of the requirements of the M. Tech degree, Department of Civil Engineering, Indian Institute of Technology Madras, Chennai, India
17. Miura N, Sakai A, Taesiri Y, Yamanouchi T, Yasuhara K (1990) Ploymer grid reinforced pavement on soft clay grounds. Geotext Geomembr 9(1):99–123
18. Montanelli F, Zhao A, Rimoldi P (1997) Geosynthetic-reinforced pavement system: testing & design. In: Proceedings of conference on geosynthetics. Industrial Fabrics Association International (IFAI), Roseville, MN, pp 619–632
19. Kinney TC, Abbott J, Schuler J (1998) Benefits of using geogrids for base reinforcement with regard to rutting. Journal of the Transportation Research Board, 1611, Transportation Research Record, National Research Council, pp 86–96
20. Moghaddas-Nejad F, Small JC (1996) Effect of geogrid reinforcement in model track tests on pavements. J Transp Eng 122(6):468–474
21. Abu-Farsakh MY, Chen Q (2011) Evaluation of geogrid base reinforcement in flexible pavement using cyclic plate load testing. Int J Pavement Eng 12(3):275–288
22. Hufenus R, Rueegger R, Banjac R, Mayor P, Springman SM, Bronnimann R (2006) Full scale field tests on geosynthetic reinforced unpaved roads on soft subgrade. Geotext Geomembr 24(1):21–37
23. Mamatha KH, Dinesh SV (2018) Evaluation of strain modulus and deformation characteristics of geosynthetic reinforced soil – aggregate system under repetitive loading. Int J of Geotech Eng, 12 (6):546-555.
24. Giroud JP, Ah-Line C, Bonaparte R (1985) Design of unpaved roads and trafficked areas with geogrids. In: Proceedings of symposium on polymer grid reinforcement. Science and Engineering Research Council and Netlon Ltd., London, pp 116–127
25. Berg RR, Christopher BR, Perkins SW (2000) Geosynthetic reinforcement of the aggregate base course of flexible pavement structures. GMA white paper II, Geosynthetic Material Association, Roseville, MN
26. Al-Qadi IL, Dessouky SH, Kwon J, Tutumluer E (2008) Geogrid in flexible pavements: validated mechanism. Journal of the Transportation Research Board, 2045, Transportation Research Record, National Research Council, pp 102–109
27. Webster SL (1993) Geogrid reinforced base courses for flexible pavements for light aircraft, test section, construction, behaviour under traffic, laboratory tests and design criteria. Report no. GL-93-6, U.S. Army Corps of Engineers, Waterways Experiment Station, Vicksburg, Mississippi, USA
28. Collin JG, Kinney TC, Fu X (1996) Full scale highway load test of flexible pavement system with geogrid reinforced base courses. Geosynth Int 3(4):537–549
29. Kwon J, Kim M, Tutumluer E (2005) Interface modelling for mechanistic analysis of geogrid reinforced flexible pavements. In: Proceedings of the conference geofrontiers, geotechnical special publication 130. Advances in Pavement Engineering, Austin, Texas
30. Perkins SW, Ismeik M (1997) A synthesis and evaluation of geosynthetic-reinforced base course layers in flexible pavements: part I experimental work. Geosynth Int 4(6):549–604
31. Qian Y, Tutumluer E, Huang H (2011) A validated discrete element modelling approach for studying geogrid—aggregate reinforcement mechanisms. In: Proceedings of geofrontiers—advances in geotechnical engineering. Geotechnical special publication no. 211, American Society of Civil Engineers, Reston, VA
32. Degroot MT (1986) Woven steel cord networks as reinforcement of asphalt roads. In: Proceedings of 3rd international conference on geotextiles, Vienna, pp 113–118
33. Kamel MA, Chandra S, Kumar P (2004) Behaviour of subgrade soil reinforced with geogrid. Int J Pavement Eng 5(4):201–209
34. Saad B, Mitri H, Poorooshasb H (2006) 3D FE analysis of flexible pavement with geosynthetic reinforcement. J Transp Eng 132(5):402–415
35. Al-Qadi IL, Tutumluer E, Kwon J, Dessouky S (2007) Accelerated full scale testing of geogrid reinforced flexible pavements. 86th TRB meeting, paper no. 07-2317, Transportation Research Board, National Research Council, Washington, DC
36. Das BM, Shin EC (1994) Strip foundation on geogrid-reinforced clay: behaviour under cyclic loading. Geotext Geomembr 13(10):657–666
37. Ibrahim EM, El-Badawy SM, Ibrahim MH, Gabr A, Azam A (2017) Effect of geogrid reinforcement on flexible pavements. Innov Infrastruct Solut 2(1):54
38. ASTM D 2487 (2011) Standard practice for classification of soils for engineering purposes (unified soil classification system). ASTM International, West Conshohocken
39. ASTM D 3282 (2009) Standard practice for classification of soils and soil-aggregate mixtures for highway construction purposes. ASTM International, West Conshohocken
40. MoRT&H (2013) Ministry of road transport and highways: specifications for roads and bridges, 5th edn. Indian Roads Congress, New Delhi
41. IRC: SP: 72 (2007) Guidelines for the design of flexible pavements for low volume rural roads. The Indian Roads Congress, New Delhi
42. Hegde A, Sitharam TG (2016) Behaviour of geocell reinforced soft clay bed subjected to incremental cyclic loading. Geomech Eng 10(4):405–422
43. IS: 5249 (2006) Determination of dynamic properties of soil—method of test. Bureau of Indian Standards, New Delhi
44. Mamatha KH, Dinesh SV (2017) Performance evaluation of geocell reinforced pavements. Int J Geotech Eng. https://doi.org/10.1080/19386362.2017.1343988
45. IRC: 115 (2014) Guidelines for structural evaluation and strengthening of flexible road pavements using falling weight deflectometer (FWD) technique. The Indian Roads Congress, New Delhi
46. IRC: SP: 20 (2002) Rural roads manual. The Indian Roads Congress, New Delhi
47. Madhavi Latha G, Nair AM, Hemalatha MS (2010) Performance of geosynthetics in unpaved roads. Int J Geotech Eng 4:151–164
48. Sireesh S, Vijay KR, Suraj V (2013) Evaluation of rutting behaviour of geocell reinforced sand subgrades under repeated loading. Indian Geotech J 45(4):378–388
49. Madhavi Latha G, Nair AM (2014) Geosynthetics in unpaved roads. Indian J Geosynth Ground Improv 3(2):3–13
50. Qian Yu, Han J, Pokharel SK, Parsons RL (2013) Performance of triangular aperture geogrid reinforced base course over weak subgrade under cyclic loading. Mater Civ Eng 25(8):1013–1021